10ème Congrès Français d'Acoustique
Lyon, 12-16 Avril 2010

Predictions Of The Unsteady Acoustic Source And Self-Noise Of A Katana Blade

L. Corriveau*[1], S. Moreau[1], J. Christophe[2], M. Roger[3]

[1] Université de Sherbrooke, 2500 Boul. De l'Université, Sherbrooke, J1K 2R1, Canada, Stephane.Moreau@USherbrooke.ca
[2] Von Karman Institute for Fluid Dynamics, 72 Chaussée de Waterloo, 1640 Rhode-St-Genèse, Belgium, julien.christophe@vki.ac.be
[3] Ecole Centrale de Lyon, 36 avenue Guy de Collongue, 69134 Ecully Cedex, France, michel.roger@ec-lyon.fr

Recently Roger [3] has studied a Katana blade. The latter is the name of the traditional single-edge, slightly curved sword used in Japanese martial arts for which different configurations of the back-edge exist, with and without grooves. The bluntness is responsible for the acoustic signature referred as the vortex-shedding and the grooves are adding high-frequency sound (cavity-tones). Lately, Roger made acoustic measurements on several Katana configurations with a wind tunnel jet velocity varying from 12 to 35 m/s yielding both low Reynolds and Mach numbers. The present work is a first attempt at deciphering the various noise mechanisms at hand observed in the above measurements achieved by M. Roger. It focuses on the comparison between two configurations of the Katana blade at a single incidence of 0° and 35 m/s: a case with two symmetric grooves and another one with a single groove. In a first step, we used Fluent 6.3 with a k-ω SST turbulence model to make a complete modeling of the small ECL anechoic wind tunnel in a RANS simulation. Then, a 3D mesh has been generated and a full 3-D LES is performed on the blade, using the boundary conditions extracted from the RANS calculation. From the LES solution we proved that a numerical LES approach to simulate the flow over a katana blade is possible and that the obtained PSD were coherent with the previous noise measurements.

1 Introduction

Small-scale unsteady flows developing in the trailing-edge region of the blades generate noise. The latter, also called self-noise, is the minimum noise a fan radiates, when free of any installation effect inducing upstream disturbances, or of any tip effect. This noise can be split into two different mechanisms, namely trailing-edge noise and vortex-shedding noise. Trailing-edge noise is associated with the convection of blade boundary-layer disturbances past the trailing edge. Vortex-shedding noise is due to the formation of a more or less organized von Kármán vortex street in the near wake. The present paper is dealing with the experimental study and numerical prediction of both noise mechanisms, ignoring other contributions. A special focus is put on the vortex shedding sound given the configuration described below. In [1-2], Roger *et al* proposed an analytical model for this noise source and provided a first validation by successfully comparing with experimental data collected on an instrumented thick flat plate at low angle of attack and low speed in the large anechoic wind tunnel at Ecole Centrale de Lyon (ECL).

2 Experimental Database

Recently Roger [3] has studied another configuration with a larger blunt trailing edge: a Katana blade. The latter is the name of the traditional single-edge, slightly curved sword used in Japanese martial arts. When the Katana is handled for cutting, the blade is moved through the air at a relatively high speed and a hiss or hushing sound can be heard. This sound depends on the angle of attack, the flow speed and the blade-profile design. The basic cross-section of a Katana blade involves a single cutting edge and a blunt back-edge similar to the base of a ballistic projectile, as shown in Fig. 1. The traditional design involves a middle ridge or *Shinogi*. The bluntness is responsible for the formation of a von Karman vortex street in the wake of the blade, and for the corresponding acoustic signature referred as the vortex-shedding sound seen around 960 Hz in Fig.2. Furthermore, some Katanas are designed with so-called 'blood-grooves' along the flat surface behind the shinogi, named *shinogi-ji* (Fig.1-bottom). These grooves are equivalent to two-dimensional cavities under a grazing flow. Therefore cavity tones are generated, due

to the instabilities of the free shear layers detaching from the upstream edges (A) of the grooves and impinging on the downstream edges (B), as generally observed for shallow cavities. This second mechanism, the groove-tones or cavity-tones is responsible for the high-frequency sound observed in Fig. 2 around 6 to 8 kHz. In [3], Roger made acoustic measurements on several Katana configurations starting with a mock-up of chord length c = 6 cm and a back-edge thickness h = 1 cm, with two symmetric grooves. An asymmetric single-groove and a no-groove configuration were also considered. The wind tunnel jet velocity was varied from 12 to 35 m/s yielding both low Reynolds and Mach numbers. The angle-of-attack was also varied yielding the interesting radiation maps, with the various tones that were attributed to cavity noise, vortex shedding noise and Tollmien-Schlichting instabilities and possible coupling between them depending on the flow condition. For the present study, the Katana mock-ups will be instrumented with remote microphone probes to provide additional wall pressure measurements and some insight on the noise sources in the simulated cases described below.

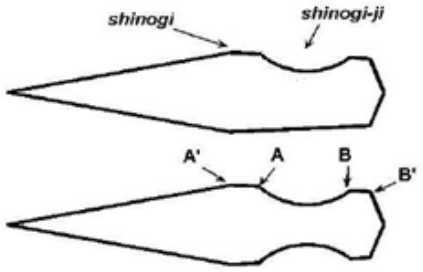

Figure 1 : Katana-blade profiles investigated in the present study, without groove (top) and with groove between edges A and B (bottom).

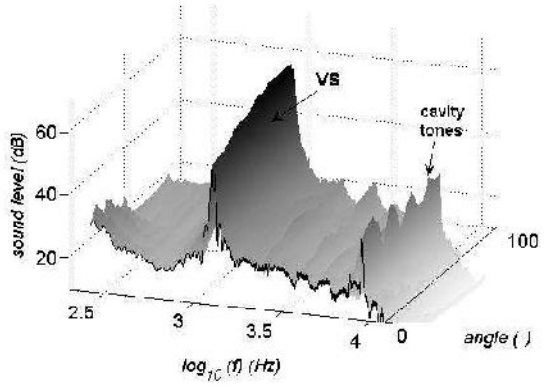

Figure 2 : Typical acoustic signature of a real Katana blade in wind-tunnel testing, in the frequency-radiation angle plane. Profile with symmetric grooves. Flow speed 24m/s.

3 LES Flow Computation

3.1 Flow Solver

The LES is based on the spatially filtered, incompressible Navier-Stokes equations with the dynamic Smagorinsky subgridscale model. Equations are solved with the commercial finite volume solver Fluent 6.3 using schemes that are second-order accurate in space and time. Preliminary RANS computations are required to provide the LES boundary conditions for computations, as described in the next section. These are performed using the Shear-Stress-Transport (SST) k-ω turbulence model, with again second order accurate solution for all variables.

3.2 Grid Topologies and Boundary Conditions

The computational procedure pursued here is the one that has been used by Moreau *et al.* [4] and Wang *et al.* [5-6] who found that wind tunnel installation effects have a significant influence not only on the airfoil loading, but also on the noise radiation. In a first step, the complete mesh of the small ECL anechoic wind tunnel is simulated by a RANS computation, including the nozzle and the Katana blade. From this solution, the correct boundary conditions are extracted for a simplified run on a truncated domain. Second, a RANS computation is performed on the truncated domain (grid extracted from the full domain), using the correct inflow boundary conditions obtained from the first run. Third, the truncated RANS domain is extruded in the spanwise direction and a full 3-D LES is performed on the katana, again using the RANS inflow conditions. The computational domain size for the LES and the incidence has been chosen so that the nozzle shear layers do not have to be resolved in the grid. The Katana blade is therefore ideally placed in the potential core of the jet. Such a methodology was successfully achieved for various airfoils in a broad range of flow conditions [7-9].

The RANS computations have shown that the flow was very similar in the two configurations for a speed of 35 m/s and a chord of 57 mm. The Fig. 3 represents the C_p which is exactly the same for the symmetric and asymmetric blades for the exception of the small zone where there is no cavity on the latter. Next, the Fig. 4 shows a zoom of the

contours of velocity magnitude on the katana which reiterate the fact that the flows are similar on the two cases.

The low Reynolds number and the large jet width to chord ratio in the present experiment allows a computational domain around the full blade. The size of the computational domain is : 2.4 C in the streamwise (x) direction, 1 C in the crosswise (y) direction and 0.1 C in the spanwise (z) direction.

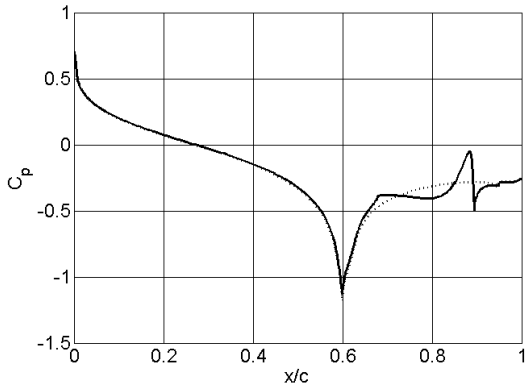

Figure 3 : Wall-pressure coefficient C_p along all katana surface for both RANS computations: (plain) symmetric profile and (dot-dot) Asymmetric profile.

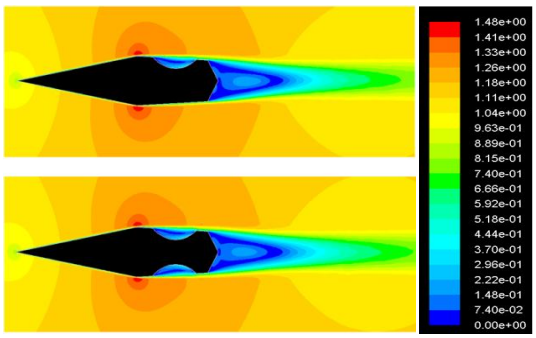

Figure 4 : Velocity magnitude contours. (top) one groove configuration and (bottom) two grooves configuration.

The resulting LES grid is a two block box mesh, with 1 250 000 cells for the coarse mesh and 4 204 550 cells for the refined mesh. The first block is completely structured and contains the katana, the other one is an unstructured enlarging of the mesh to capture the vortices in the wake while not having too many cells. The LES use a no-slip boundary condition on the blade surface, a pressure outflow boundary condition at the exit plane, and the steady RANS velocity (U and V) along the upper and lower boundaries. Periodic boundary conditions are applied in the spanwise direction. Computations were run for at least 5 flow-through times, based on the free stream velocity and blade chord length, before a statistically steady state was reached and mean values were collected. Airfoil surface pressure and wake velocity statistics were then acquired for a period of at least 4 flow-through with a sampling rate of 120 kHz.

3.3 Results

The present work is indeed a first attempt at deciphering the various noise mechanisms at hand observed in the above measurements achieved by Roger [3]. Yet, the present results focus on the noise sources only. The flow over the Katana blade at a single incidence of 0° is compared between a case with two symmetric grooves after the shinogi and another one with a single groove yielding an asymmetric configuration. We also want to make an analysis on the effect of the grid density on the solution, but since we have not finished the data collecting on our high density mesh, we can't provide an accurate analysis in this paper.

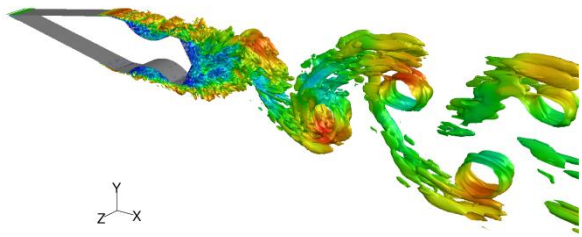

Figure 5: Flow topology of the two grooves configuration katana blade described by the Q-factor.

The flow topology is first illustrated in Fig. 5 by the isocontours of constant Q factor, which show the level of vorticity and the size of the turbulent structures in the flow at a given instant. It shows that the LES on the symmetric two-groove configuration is showing well-developed turbulent structures. Transition occurs just after the Shinogi with initial rollers breaking down at the cavity edge. From this separation point, the shear layer oscillates over the cavity, shedding small structures that impact the opposite side of the cavity (peak in the pressure coefficient in Fig. 7). Additional small structures build up till the trailing edge. The flow separates and forms large vortical structure typical of the vortex shedding process in the wake. The two long

structures (like “legs”) connect alternating vortices. The comparison between the LES on the two Katana configurations enabled us to confirm similar structures in the asymmetric case.

The lift convergence curve shown in Fig. 6 proves that the flow is stabilized and out of the transition state. By comparing the two configurations, their intensities are seen to be very close, but the two signals are in exact opposite phase. This means that the von Karman vortex street in the wake of the blade is inverted in the two cases. More importantly, we see that the frequency of the oscillations is the same for the two cases, which means that having one or two grooves has no impact on the Von Karman frequency.

As a statistically steady state was reached, means values were collected. The mean and fluctuating wall-pressure were analyzed for each of the LES runs. The mean pressure on the surface, characterized by the pressure coefficient $\bar{C}$p, is shown in Fig. 7. The graph shows some major differences in the flow between the two katana configurations. There is a separation of the flow at A’(Fig. 1) on the asymmetric blade while there is none on the other one. There is also a similar but smaller separation on the filled side without cavity. This phenomenon has been confirmed by the mean velocity contours. The grid might be too coarse and might induce perturbations in the boundary layer and provoke a separation, which was not seen in the previous RANS computations as seen in Fig. 3. Future experimental measurements will confirm the existence or not of the recirculation bubbles.

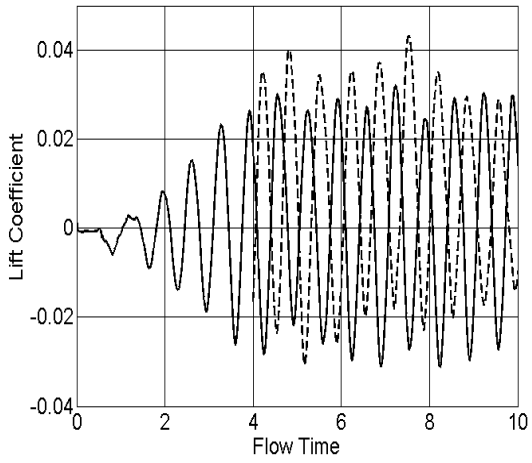

Figure 6 : Lift coefficient time convergence for both computations: (plain) symmetric profile and (dash) asymmetric profile.

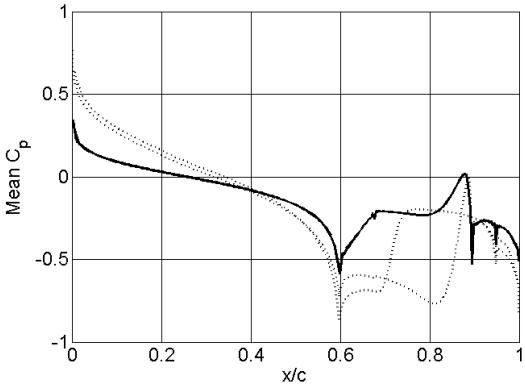

Figure 7 : Mean wall-pressure coefficient $\bar{C}_p$ along all katana surface for both LES computations: (plain) symmetric profile and (dot-dot) Asymmetric profile.

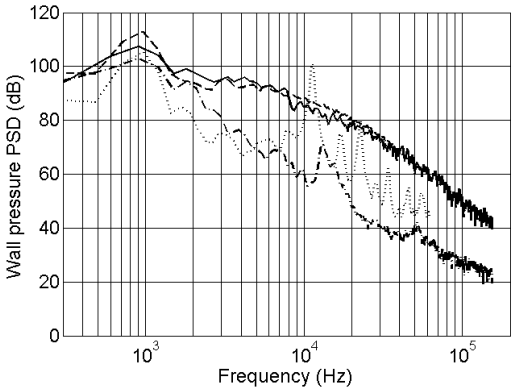

Figure 8 : Frequency spectra of the wall pressure fluctuations on the suction side near the trailing edge (x/C=0.9): (plain) symmetric profile and (dash) asymmetric profile and just before the groove (x/c=0.63): (dash-dot) symmetric profile and (dot-dot) asymmetric profile.

The wall-pressure spectra near the trailing edge are then compared between both katana configurations. The global shape of the curves is very similar in both case and is as expected from the work of Roger [3]. There is a high-intensity peak just before 1 kHz representing the vortex shedding noise and we see the broadband noise from the blunt trailing edge on the full spectrum. Then, there is another peak seen on the probe just before the groove around 10 kHz representing the cavity tone. This tone is present in both configuration but is more intense on the two grooves profile. Again, future experimental measurements will be able to assess the accuracy of the simulation.

Fig. 9 shows the mean and rms of the velocity magnitude at four different measurement stations from x/C = 1.0574 to x/C = 1.1686. For all stations, computations present very similar shapes with a wake deficit. The double-peak in (a) and (b) is due to passage of the stations in the recirculation bubble near the blunt trailing edge of the katana. While in (c) and (d), we are out of this recirculation bubble and see a classical wake velocity profile with a speed deficit behind the blade. Every velocity profile is centered on y=0, which is coherent with our angle of attack of 0°. Finally, on all rms velocity profile, we notice a small shift between the two cases; the asymmetric curve is slightly higher in the graphs than the other one, which is the only trace of the geometric difference between the blades.à

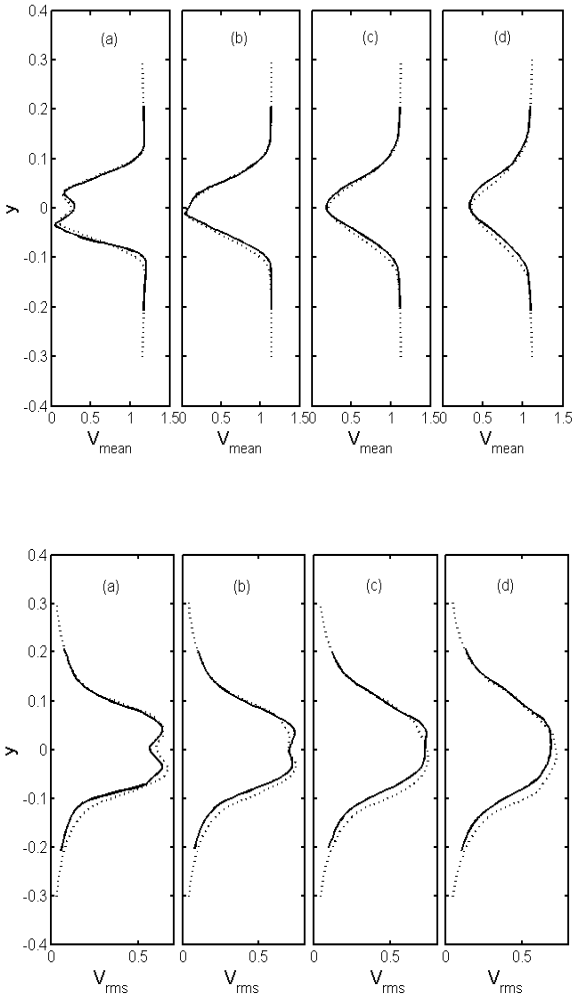

Figure 9 : Wake velocity data. (top) Mean velocity magnitude and (bottom) RMS velocity magnitude at four x/C locations : (a) x/C = 1.0574, (b) x/C = 1.0940, (c) x/C = 1.1313 and (d) x/C = 1.1686. (plain) asymmetric profile and (dot-dot) symmetric profile.

4 Concluding Remarks

The present paper has proven that a numerical LES approach to simulate the flow over a katana blade was possible and that the obtained PSD were coherent with the previous noise measurements by Roger [3]. The next step will be to define the effect of the grid density on the flow solution. Then, a coherence analysis will be made to know if the spanwise extent of 0.1c is enough to capture the spanwise coherence length properly. Finally, comparisons with future measurements of the wall pressure statistics should help validating the mean loading and pressure fluctuations found on the Katana blades. In turn, both the pressure and velocity statistics found close to the trailing edge will be used as inputs to the trailing-edge model proposed by Roger *et al* [10] to compare with the previous acoustic measurements. The flow structure seen in Fig. 5 already suggests that this configuration should provide a proper test case for the analytical vortex-shedding noise model proposed by Roger et *al* [1-2].

Acknowledgments

L. Corriveau is thankful to the Université de Sherbrooke for giving him the opportunity to make this research project, to the RQCHP for letting him use the Mammouth cluster for all of his computation and to all of his colleagues who has given him a necessary support.

References

[1] M. Roger, S. Moreau & Y.J. Moon – *Fan broadband noise prediction using hybrid methods and analytical modeling*. Proceedings of the INTER-NOISE-2006 conference, Honolulu, Hawaii (2006).

[2] M. Roger, S. Moreau & A. Guédel – *Vortex-Shedding Noise and Potential-Interaction Noise modeling by a Reversed Sears' Problem*. AIAA 2006-2607 paper, Cambridge (2006).

[3] M. Roger – *Coupled oscillations in the aeroacoustics of a Katana blade*. Proceedings of Acous'08 conference, Paris, France (2008).

[4] S. Moreau, M. Henner, G. Iaccarino, M. Wang & M. Roger – *Effect of Airfoil Aerodynamic Loading on Trailing-Edge Noise Sources*. AIAA J., Vol. 41 (10) (2003).

[5] M. Wang, S. Moreau, G. Iaccarino, & M. Roger – *LES Prediction of Pressure Fluctuations on a Low Speed Airfoil*. Annual Research Briefs 2004. Center for Turbulence Research, Stanford, California (2004).

[6] M. Wang, S. Moreau, G. Iaccarino & M. Roger – *LES prediction of wall-pressure fluctuations and noise of a low-speed airfoil*. International J. Aeroacoutics, Vol. 8 (3) (2009).

[7] J. Christophe, J. Anthoine & S. Moreau – *Trailing Edge Noise of a Controlled-Diffusion Airfoil at Moderate and High Angle of Attack*. AIAA 2009-3196 paper, Miami (2009).

[8] J. Winkler, S. Moreau & T. Carolus – *Large-Eddy Simulation and Trailing-Edge Noise Prediction of an Airfoil with Boundary-Layer Tripping*. AIAA 2009-3197 paper, Miami (2009).

[9] S. Moreau, M. Roger & J. Christophe – *Flow Features and Self-Noise of Airfoils Near Stall or Stall*. AIAA 2009-3198 paper, Miami (2009).

[10] M. Roger & S. Moreau – *Back-scattering correction and further extensions of Amiet's trailing-edge noise model. Part 1: theory*. Journal of Sound and Vibration 286 (477-506) paper (2005).